

MORPHOLOGICAL CHARACTERIZATION OF AN EXCEPTIONALLY PRESERVED EOLIAN SYSTEM: THE CRETACEOUS TRONCOSO INFERIOR MEMBER IN THE NEUQUÉN BASIN (ARGENTINA)

Agustín Argüello Scotti¹, Gonzalo D. Veiga¹

¹ Centro de Investigaciones Geológicas (CONICET-Universidad Nacional de La Plata). Diagonal 113 esquina 64, La Plata (B1900TAC), Buenos Aires, Argentina. aarguello@cig.museo.unlp.edu.ar, veiga@cig.museo.unlp.edu.ar

ARTICLE INFO

Article history

Received June 2, 2015

Accepted November 11, 2015

Available online November 23, 2015

Handling Editor

Diana Cuadrado

Keywords

eolian dune

preserved topography

3D modeling

Troncoso Inferior Member

Neuquén Basin

ABSTRACT

The aim of this study was to characterize in detail the exceptionally preserved eolian morphology within the uppermost section of the Lower Cretaceous Troncoso Inferior Member at the classic outcrop locality of Loma La Torre in northern Neuquén, Argentina. The major motivations for this work are to provide new perspectives on the current knowledge of the system at this locality and to analyze the implications of a detailed study for the adequate construction of subsurface models. The Troncoso Inferior Member is one of the most important conventional hydrocarbon reservoirs in the Neuquén Basin. In the northern Neuquén province, its upper section is characterized by the preservation of an eolian dune field, with the best reservoir properties, overlain by marine evaporites. The elaboration of a detailed stratigraphic framework was successful in identifying multiple independent eolian sequences and allowed the isolation of the last eolian event, responsible for the preserved morphology. A combination of several surveying methods, including total station and 3D photogrammetry-based models, were used for a precise mapping of stratigraphic surfaces across a 7.5-km-long section. The resulting dataset was analyzed within RMS© software, which provided multiple realizations of depth and thickness maps. Results revealed a system of dunes and draas of linear type and a WSW-ESE orientation, associated with small-scale features both superimposed to the main bedforms and in the interdune areas. Measurements of morphological parameters of the major bedforms, including spacing, width and height, along with interdune width, were performed. Comparison with a modern-day analog of similar scale and characteristics provided valuable insights on the environmental conditions which constrained this system and the singularities of its construction, accumulation and preservation. Our results suggest that these dunes underwent construction under dry conditions and a limited supply or availability of sand, most likely under a bimodal wind regime, and that their preservation is entirely related to subsequent marine transgression. Moreover, this study highlights that modeling this unit in the subsurface with the detail required for managing mature fields requires a very good understanding of the system evolution.

INTRODUCTION

Although numerous studies have described the exceptional preservation of ancient dune field morphology (Glennie and Buller, 1983; Clemmensen, 1989; Benan and Kocurek, 2000; Jerram *et al.*, 2000; Scherer, 2002; Strömbäck and Howell, 2002), few have provided a detailed quantification of such preserved geometries. In the case of the Troncoso Inferior Member in the Neuquén Basin, the eolian morphology preserved at the top of the unit is of great economic importance, given that this interval constitutes one of the most important conventional hydrocarbon reservoirs of the basin. In this regard, production and reserve calculations are greatly influenced by characterization and modeling of the preserved morphology (Dajczgewand *et al.*, 2006). Its determination in the subsurface however, is far from a simple task. First, the seismic response of the interval is masked by a 20-meter-thick anhydrite layer of regional extension, lying directly over the eolian deposits (Masarik, 2002). Secondly, the thickness of fluvial sandstones below the eolian interval can have considerable variations in short distances thus making the seismic amplitude maps harder to interpret. In addition, in the outcrops corresponding to this interval, Veiga *et al.* (2005) have identified two superimposed independent eolian sequences, suggesting that the identification and mapping of previous eolian sequences could be a key factor for a precise reconstruction of the final morphology of the system. In this context, the available outcrops of this unit provide an excellent opportunity to map the morphology of the dunes within a robust stratigraphic and sedimentological framework. Therefore, the aims of this work are (i) to characterize the detailed morphology of the dunes in the classic locality of Loma La Torre, (ii) to discuss the impact of the observed morphology on the current understanding of the system at this locality, and (iii) to analyze the implications of a detailed reconstruction of the preserved morphology for the adequate construction of subsurface models.

GEOLOGICAL SETTING

The Troncoso Inferior Member of the Huitrín Formation is part of the sedimentary infill of the Neuquén Basin, a major depocentre developed in western Argentina over a long history spanning

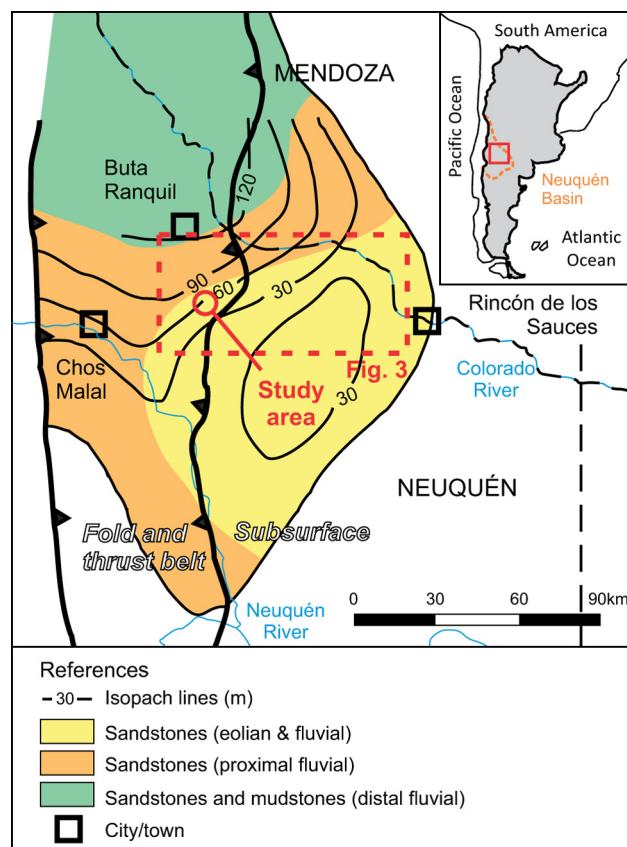


Figure 1. Areal distribution and thickness of the Troncoso Inferior Member along with its characteristic lithologies and interpreted depositional environments (modified from Veiga and Vergani, 2011).

from late Triassic to early Paleogene times (Howell *et al.*, 2005). The distribution of the Troncoso Inferior comprises the northern Neuquén and southern Mendoza provinces (Fig. 1). It is interpreted as originated entirely in continental clastic environments, representing a major relative sea-level fall during the Barremian that led to a total disconnection of the basin from the proto-Pacific Ocean (Legarreta, 2002; Veiga and Vergani, 2011). The unit overlies the marine deposits of the Agua de la Mula Member (Agrido Formation) and Chorreado Member (Huitrín Formation) across a regional unconformity, and is separated from the overlying marine evaporitic deposits of the Troncoso Superior Member by a major flooding surface (Fig. 2). Veiga *et al.* (2005) carried out the regional sedimentological analysis of this interval relating the deposition of this unit to a complex arrangement of braided fluvial, mixed-load ephemeral fluvial, eolian and lacustrine environments. In the northeastern sector

of the basin, this unit is characterized by sandstones related to the development of a vast eolian dune field, overlying braided fluvial deposits or, in some cases, directly on top of previous marine strata. The final morphology of this dune field is partially preserved due to the abrupt flooding of the basin and the subsequent deposition of evaporites. The flooding event was accompanied by partial deformation and reworking of eolian sand, previously studied by Strömbäck *et al.* (2005). The dune field is mainly distributed within the subsurface of the Neuquén province, where it comprises the main reservoir to numerous oil fields. Furthermore, in the easternmost sector of the Agrío fold and thrust belt, this ancient erg is exposed along a series of excellent outcrops of considerable continuity which may provide good analogies for subsurface scenarios.

The outcrops of the Troncoso Inferior Member at the Loma La Torre (also known as Barda Atravesada) have been traditionally regarded as suitable analogs to assist subsurface reconstructions. They comprise a series of cliffs that mark the southern limit of the Pampa de Tril plain located in northwestern Neuquén (Fig. 3). They are clearly visible from the national road n°40, halfway between the localities of Chos Malal and Buta Ranquil, and are easily accessible through provincial roads n°6 and 9. These outcrops lie 40 to 70 km west of the major oilfields (e.g. Chihuido de la Sierra Negra, El Trapial and Puesto Hernández, Valenzuela *et al.*, 2011) whose main hydrocarbon production comes from the eolian facies of the studied interval (Fig. 3). For the purpose of this study, a 7.5-km-long section was selected. The outcrops in this area comprise a series of nearly vertical cliffs sometimes exceeding 50 m in height and formed within the Troncoso Inferior and Superior Members, on top of a 200 meter-high talus composed of basinal deposits of the Agua de la Mula Member. While the outcrops are very continuous and stratigraphic surfaces can be mapped for several kilometers, detailed measurements in the steepest cliff sections represent a considerable logistical challenge.

METHODS

To fulfill the objectives of this study a workflow consisting of three stages was implemented: (i) a sedimentologic and stratigraphic survey, whose specific objective was to define a detailed stratigraphic

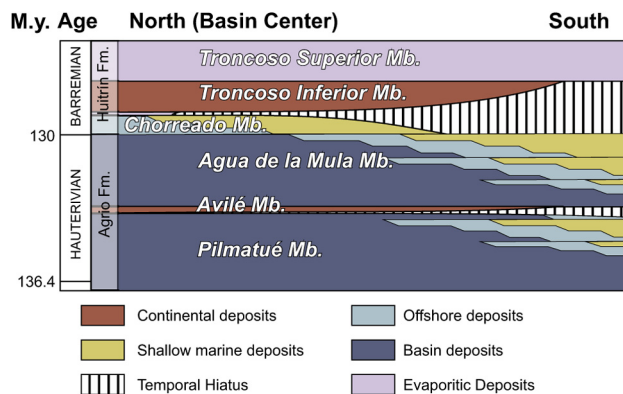


Figure 2. Hauterivian-Barremian chronostratigraphic scheme of the Neuquén Basin.

framework for the interval, (ii) a surface mapping survey, in which the surfaces defined earlier were mapped using a variety of methods, and (iii) outcrop reconstruction and analysis, which consisted in the construction of depth and thickness maps for the studied interval and the characterization and analysis of the observed morphology, followed by the identification and study of suitable modern analogs.

Definition of a high-resolution stratigraphic framework

The main interest within this stage was to isolate the youngest eolian deposits (which arguably represent the system preserved by subsequent flooding) from previous sequences. Across the study area, 23 sedimentary logs and several correlation photo-mosaics were obtained. Based on the logs and taking previous studies into account (Veiga *et al.*, 2005, Veiga and Vergani, 2011), a lithofacies scheme was developed, according to the textural properties and sedimentary structures observed in the rocks. This scheme was further organized into three facies associations. The distribution of these associations within the interval allowed the identification of the surfaces of interest for further mapping.

Stratigraphic surface mapping

Given the singularities of the outcrops, a variety of methods and tools were used to map the stratigraphic surfaces, which included: (i) traditional sedimentary logs, (ii) total station, (iii) calibrated photo-logs, and (iv) 3D photogrammetric models.

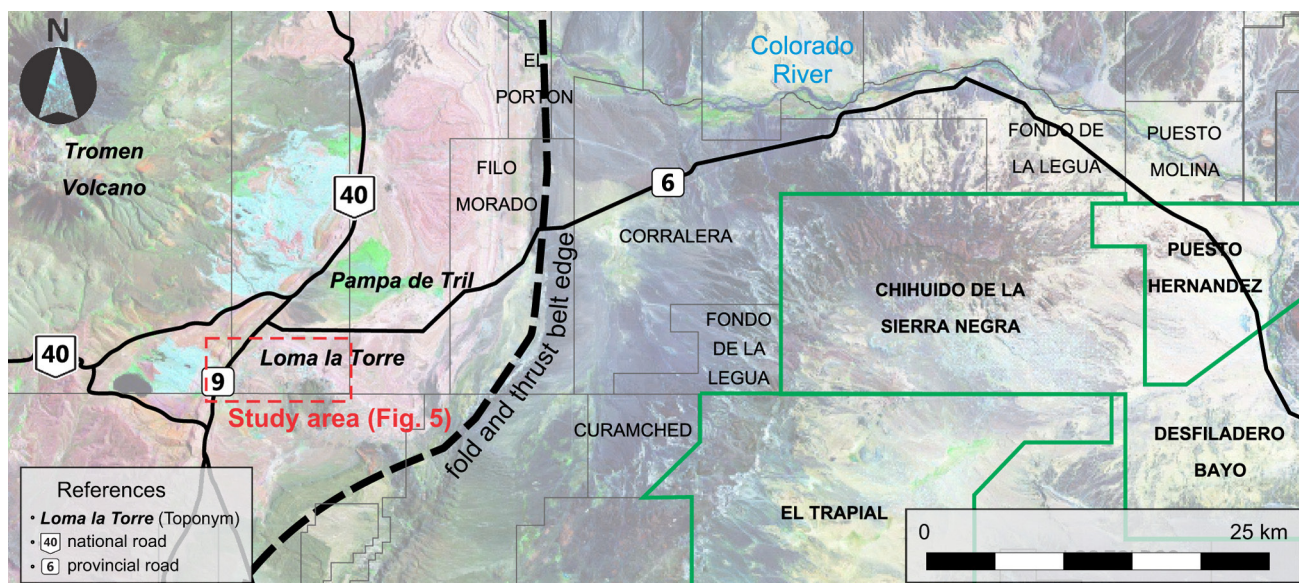


Figure 3. Landsat satellital image of the northern Neuquén Province showing the location of the study area (red dashed line) and the adjacent oilfields to the east. Oilfields in which the main hydrocarbon production comes from the eolian facies of the Troncoso Inferior Member are highlighted in green color.

Each method was used to generate point data with XYZ coordinates, representing the position of a surface in space. The data obtained from different methods was integrated with measurements from total station, which was regarded as the main tool because of its precision in both the horizontal and vertical dimensions. The XYZ coordinates and the orientation of the first station of the total station were obtained with regular GPS. The GPS error in this case is not considered relevant since a precise georeference of the model is not required. What is regarded important for the model is a precise measurement of the relative distance and orientation between mapped points.

Sedimentary logs were referenced with total station, taking the XYZ coordinates of the intersection between the surfaces and the log. Mapping with the total station's prism was carried out in all sectors accessible by foot. Although this method was very effective regarding time consumption and accuracy, it had little use for the extensive cliff sections of almost impossible access and alternative mapping methods were sought and tested. The “calibrated photo-log” (CPL) is a safe and precise method to measure logs in vertical cliffs, which was carried out following the methodology proposed by Howell *et al.* (2008). The result is a picture, vertically scaled across a graduated rope, which allows measuring

the position of any surface or feature that the rope intersects.

Another suitable solution for mapping inaccessible cliff sectors was the construction of three-dimensional digital outcrop models generated by photogrammetric methods. This method is a powerful and inexpensive resource that has flourished in recent years due to increasing processing capacity of available computers. The method consists on determining the 3D geometry of an object by taking multiple 2D photographs of it from different positions and angles. VisualSFM (structure from motion) (Wu, 2011) software was used to build a point cloud, representing the shape of the outcrop, from matching points found across a large number of digital photographs (Fig. 4a, b). This point cloud was imported into MeshLab software (Cignoni *et al.*, 2008), to create a surface which provides the best fit to the point cloud (Fig. 4c). Next, the original images were projected over the surface, giving “texture” to the latter (Fig. 4d). Finally, the modeled surface was scaled and referenced using a minimum of 4 points taken with total station on sites represented within the model. The final result is a digital model of the outcrop with an error inferior to 1 m which allows mapping surfaces and measuring all kinds of two- and three-dimensional features in both accessible and inaccessible cliff sectors.

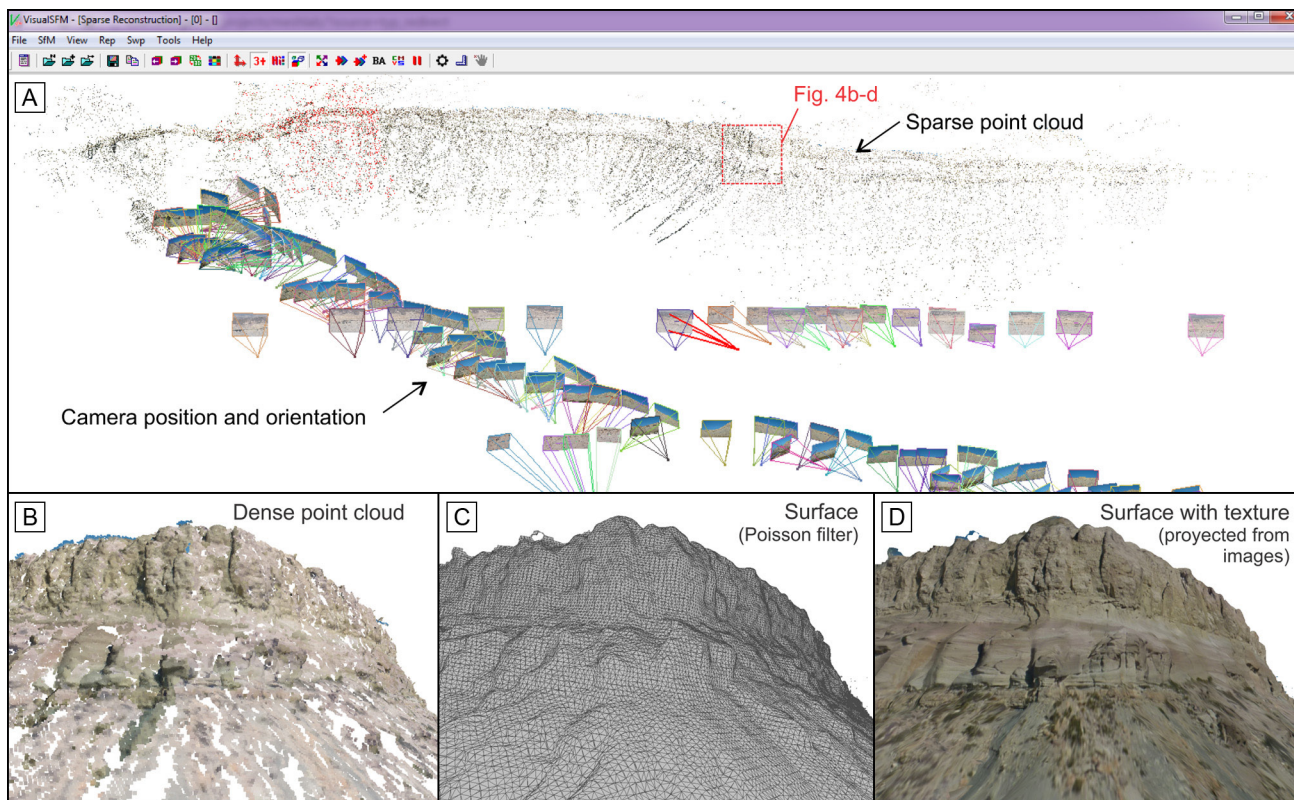


Figure 4. Workflow followed for the generation of 3D photogrammetric models. **a)** Visual SFM interface showing the results of the “compute missing matches” and “3D reconstruction” functions. **b)** Dense point cloud generated in Visual SFM and imported in MeshLab. **c)** Result of surface reconstruction from the dense point cloud using the Poisson filter. **d)** Previous surface with texture projected from the original images.

Digital outcrop model construction and morphological analysis

A point cloud was assembled using reservoir modeling software RMS©, comprising well over 600 points (Fig. 5) from all different sources (54 from sedimentary logs, 26 from CPLs, 440 from total station and 136 from photogrammetric models). Before mapping the surfaces, two different models of the outcrop were created: a deformed model was assembled from the unaltered points with the original field coordinates, and thus involving the current structural deformation of the outcrop. On the other hand, a retro-deformed model was built from the result of a structural analysis of the outcrop and a subsequent retro-deformation of the point cloud. Finally, all surfaces in the stratigraphic framework were mapped in both models with interpolation algorithms provided by RMS© (local and global b-spline, polynomial, kriging, converging average, etc.), producing depth and thickness maps of the

surfaces and the zones they bound, respectively. Using these maps the shape of the different surfaces was analyzed and measurements of the morphological parameters of the preserved dunes were performed, based on the criteria used by Al-Masrahy and Mountney (2013). A measure of flank width and dune symmetry was introduced to help defining the dune type which is not as evident in the outcrop as it is on modern active dunes. Finally, suitable modern analogs were sought to test the results and to aid further discussions about the environmental constraints to which the late Troncoso eolian system might have been subjected.

FACIES ASSOCIATIONS

The lithofacies determined for the Troncoso Inferior Member were grouped into eolian, fluvial and marine reworking facies associations, according to the broad environmental interpretation assigned to each group.

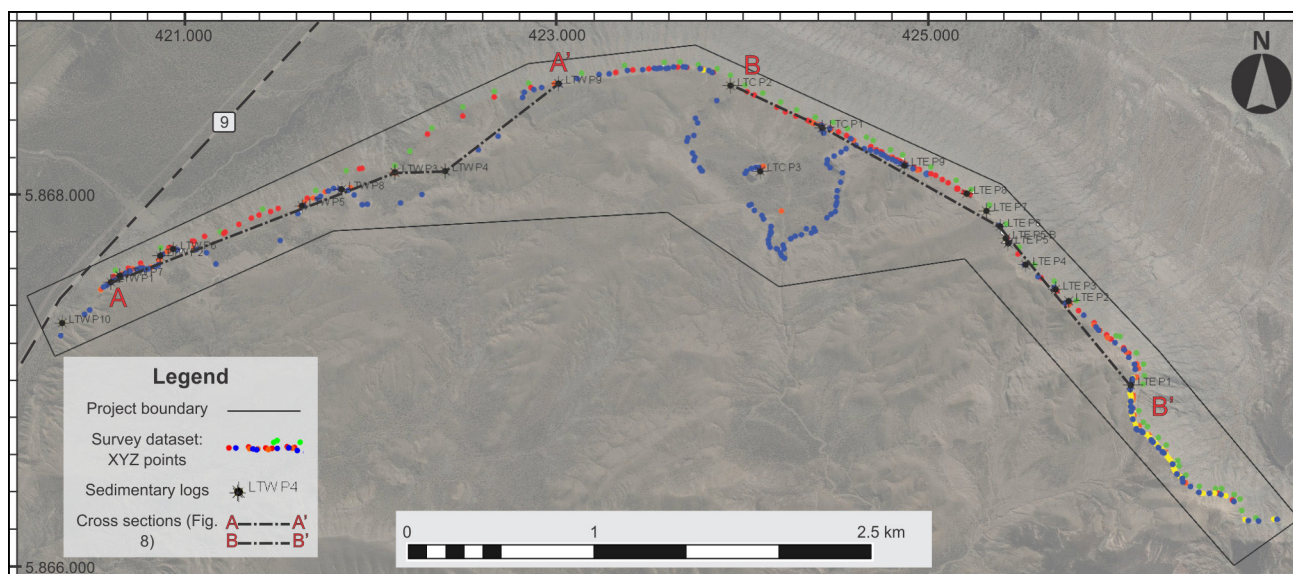


Figure 5. Study area and project's boundaries, along with the dataset generated during the field survey, superimposed onto Google Earth imagery.

Eolian Facies Association

Description. This association is almost entirely comprised by medium- to fine-grained sandstones with bedding dips ranging from steeply inclined (25-30°) to sub-horizontal. Inclined strata are composed of medium to fine sand and range in thickness from 1-6 cm (Fig. 6a). Inclined laminae, close to millimeter-thick and composed of very fine sand, are also commonly present interbedded with inclined strata (Fig. 6b). On the other hand, low-angle to sub-horizontal laminae are composed of medium- to very fine-grained sand, varying in thickness from a few grains to a few mm (Fig. 6c). Inverse grading is commonly appreciable within these laminae as their thickness reaches 1-2 mm. The last facies in this association comprises thin strata (1-3 cm thick) composed of abundant very coarse sand grains, granules and small pebbles within a medium-grained sand matrix (Fig. 6d, e).

Interpretation. The relatively thick inclined strata are interpreted as generated by grain flows or avalanches either amalgamated or separated by thin and broadly finer grained grain fall deposits (Hunter, 1977), processes associated to the lee side of eolian bedforms. Low-angle to sub-horizontal lamination is attributed to the migration of wind ripples where inverse grading is observable (climbing traslatent strata of Hunter, 1977). Where this grading is not

clearly distinguishable, the origin of these laminae may be as well related to grain fall processes. Thin beds comprising very coarse sand grains and fine-grained gravels were interpreted as the product of deflation and *in situ* concentration of particles too heavy to be carried by the wind for long distances. Depending on the type and dip angle of eolian bedding, different eolian sedimentary units were differentiated: dune core elements display variable proportions of inclined grainflow stratification and grainfall lamination, while dune plinth elements are found at the interdigitation between dune core units with low-angle, wind-ripple lamination. Interdune elements are characterized by thin sandstones with subhorizontal wind-ripple lamination and local accumulation of coarse sand clasts, while sandsheet elements have similar facies but comprise thicker (up to 1 m), more laterally extensive deposits when compared to interdunes.

Fluvial Facies Association

Description. This association is characterized by a preponderance of sandstones. Abundant coarse- to medium-grained sandstones, with sporadic coarser clasts of very coarse sand, granules and pebbles, are commonly associated with trough cross stratification (Fig. 7a), horizontal or low-angle stratification. Less common medium- to fine-grained sandstones show

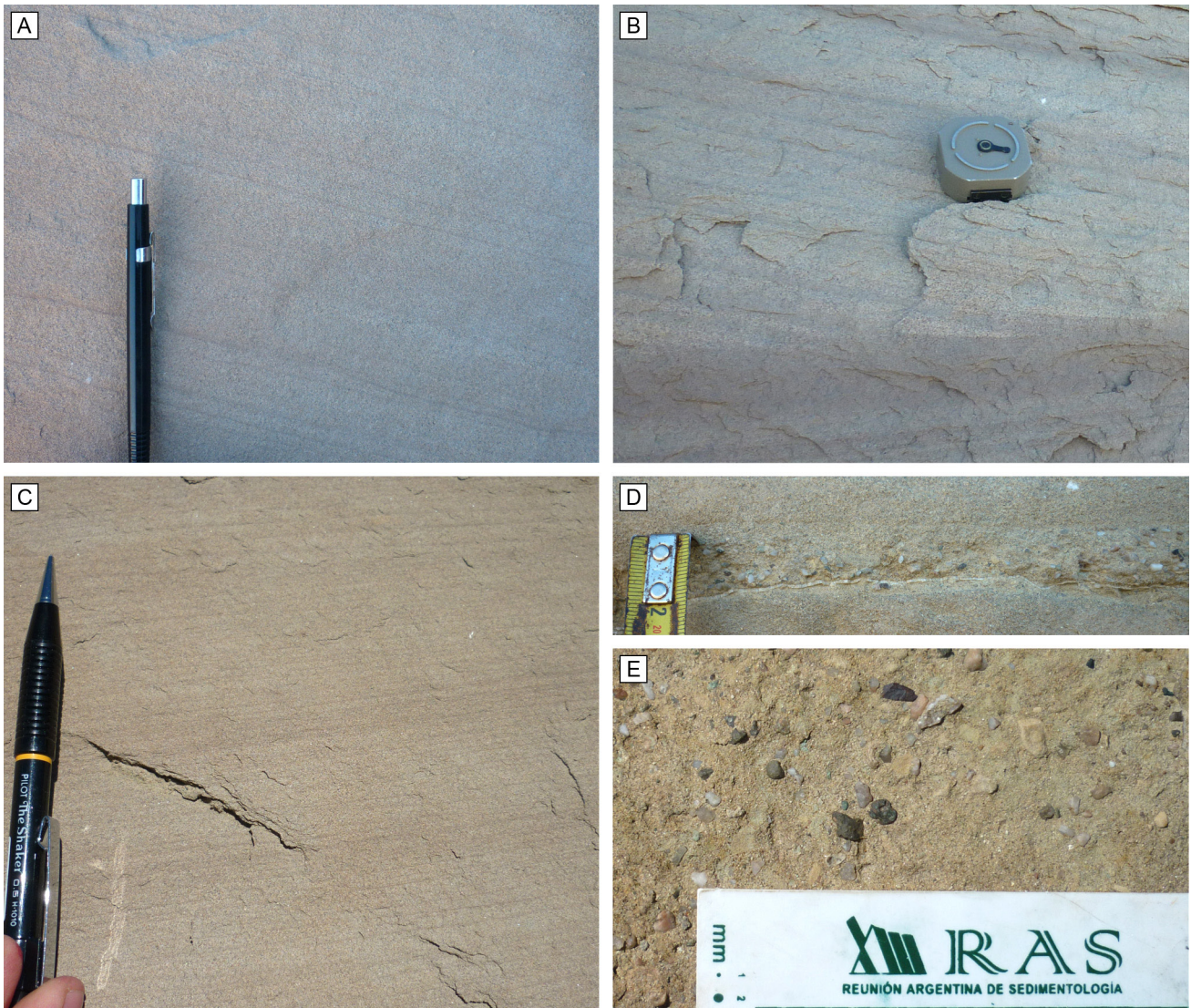


Figure 6. Eolian facies association. **a)** Grey grainflow strata of variable thickness (fine and medium sand) separated by thin grainfall laminae in dark grey color (very fine sand). **b)** Dune toe showing grainflow strata of pale yellowish grey color, many of which display clear internal inverse grading, wedging downdip within wind ripple laminae of reddish brown color. **c)** Subhorizontal wind-ripple lamination of very thin but variable thickness, showing grain size bimodality and in some cases inverse grading. Darker reddish laminae are finer grained (very fine sand) than yellowish grey laminae (fine and medium sand). **d)** Cross-section view of a thin layer consisting of coarse sand, granule and very fine pebble clasts within a medium grained sand matrix, interpreted as a concentration of coarse clasts by deflation processes. **e)** Plan view of the facies shown in figure 6d.

cross lamination, preserved ripple forms, or appear massive. The coarser sandstones are commonly associated with abundant concentration of pebble- to cobble-size intraclasts and lithoclasts of green mudstones, especially at the base of cross bedded sets. In some cases these accumulations comprise intraclast conglomerates. Subordinated green mudstone intervals of little lateral continuity are also found within the association. They are mostly massive and with desiccation cracks (Fig. 7b).

Interpretation. The coarser sandstone facies represent deposition from aqueous unidirectional and channelized flows, while the subordinated fine sandstones and mudstones represent lower energy unidirectional sheet flows, with occasional subaerial exposure and likely pedogenic processes. Coarse sandstone facies therefore represent deposition within the main channels of the system, while subordinated fine sandstones and mudstones represent overbank deposition with low preservation

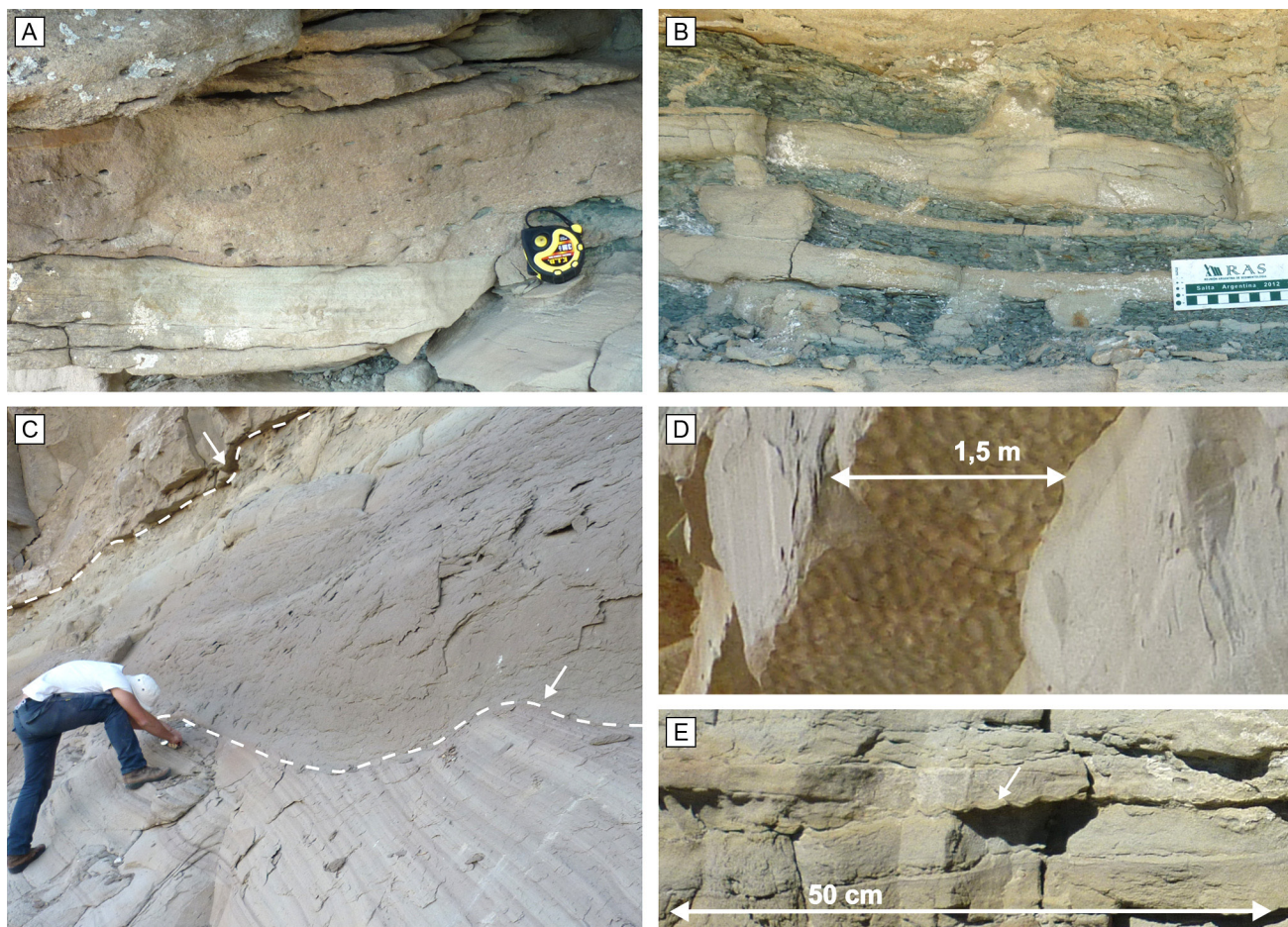


Figure 7. Fluvial and marine reworking facies associations. **a)** Cross-stratified medium- to coarse-grained sandstone with abundant green mudstone intraclasts; a recurrent facies within the fluvial facies association. **b)** Fine- to medium-grained massive sandstones interbedded with massive mudstones having desiccation cracks. **c)** Massive and faint laminated sandstones associated to resedimentation of eolian sand during the flooding of the dunes. Note the sharp contacts with the underlying eolian sandstones (lower white dashed line and arrow) and the overlying evaporites of the Troncoso Superior Member (upper white dashed line and arrow). **d)** Asymmetric ripples at the top of massive to faint laminated sandstone body. **e)** Cross-section view of symmetric wave ripples (white arrow) associated to wave action during the transgression.

potential. These processes are interpreted to have been developed within a braided fluvial system. This facies association is equivalent to the “coarse-grained braided” association described by Veiga *et al.* (2005).

Marine Reworking Facies Association

Description. This association is composed of sandstones with textural properties similar to the eolian sandstones, but mostly massive and with sub-horizontal faint lamination (Fig. 7c), or less commonly with preserved current and wave ripples (Fig. 7d, e). This association typically sharply overlies the eolian facies (Fig. 7c), and form discontinuous,

relatively thin deposits. This association also includes relatively uncommon sandstones with folded structures where bedding in the eolian facies association is recognizable, but considerably contorted. Where this deformed facies is present, the transition between the marine reworking and eolian facies associations is more gradual.

Interpretation. Most of the facies in this association are interpreted to be formed by processes related to the destabilization and resedimentation of eolian dunes in a subaqueous environment, with subordinated wave action and reworking. On the other hand, facies with folded structures are interpreted as formed by soft sediment deformation of eolian strata, generated by sudden escape of air

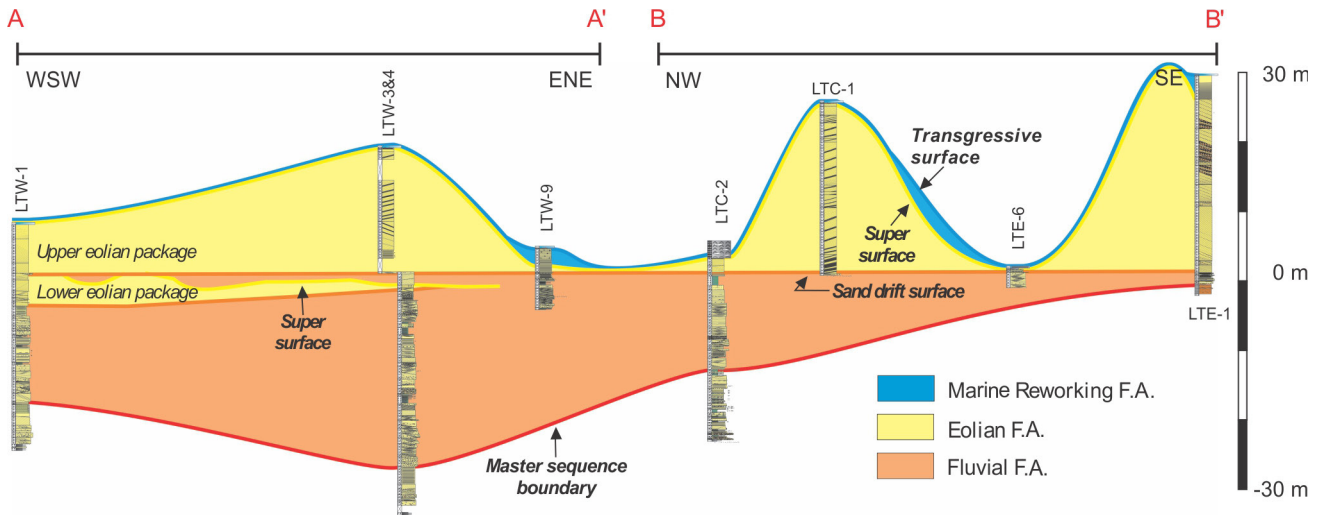


Figure 8. Stratigraphic cross-section with key sedimentological logs showing the distribution of the facies association across the study area. Logs are leveled at the base of the last eolian event (LEE).

or water. All of these processes are related to the marine flooding of the eolian dunefield. These facies and corresponding sedimentary processes have been reported and discussed in detail by Strömbäck *et al.* (2005).

FACIES DISTRIBUTION AND DETAILED STRATIGRAPHIC FRAMEWORK

The facies association distribution across the study area (Fig. 8) clearly shows that in the western sector there are two distinctive eolian packages separated by a sandy fluvial interval, as had been previously noted by Veiga *et al.* (2005). The concave basal geometry of the fluvial interval reflects incision into underlying eolian deposits, while their upper contact is characterized by a concentration of coarse sand grains, granules and pebbles, indicating the action of deflation processes (Fig. 6d, e). Locally, the two eolian packages are found directly superimposed and separated only by a sharp surface with concentration of coarse sand grains. These stratigraphic relationships support the interpretation of both packages as separate, independent eolian sequences. As for the packages themselves, each one has distinct sedimentological features, which may be helpful to aid their identification in subsurface scenarios. The lower package is coarser grained, moderately sorted, and composed of small-scale dune elements, dry interdune and sand-sheet deposits. The upper interval in contrast, is finer

grained, better sorted and characterized by large-scale dune and dry interdune elements and the absence of sand-sheet deposits.

The upper eolian package represents the youngest eolian deposits of the studied unit and as such was denominated “last eolian event” or “LEE”. In contrast to the lower eolian package, found only in the western sector, the LEE is widespread across the study area (Fig. 8), despite considerable variations in thickness. In the easternmost sector it lies directly on top of previous marine strata, suggesting an even more widespread distribution than the underlying fluvial deposits.

Following the facies association distribution, a stratigraphic framework to model the study interval was constructed (Fig. 9). Surface 0 is the lowermost surface within the studied interval and represents the top of an easily distinguishable continuous carbonate bed within the outer-ramp deposits of the underlying Agua de la Mula Mb. (Spalletti *et al.*, 2001). Even though this bed does not belong to the studied unit, it served as a nearly horizontal datum for the rest of the model. Several meters above Surface 0, Surface 1 marks the lower limit of the Troncoso Inferior Member. This surface was interpreted as a low-order master sequence boundary by Veiga *et al.* (2005). Zone A comprises the totality of sandstones and mudstones assigned to the fluvial facies association of the Troncoso Member in the study area, as well as sandstones of the eolian facies association belonging to the lower eolian package. Zone A is bounded at

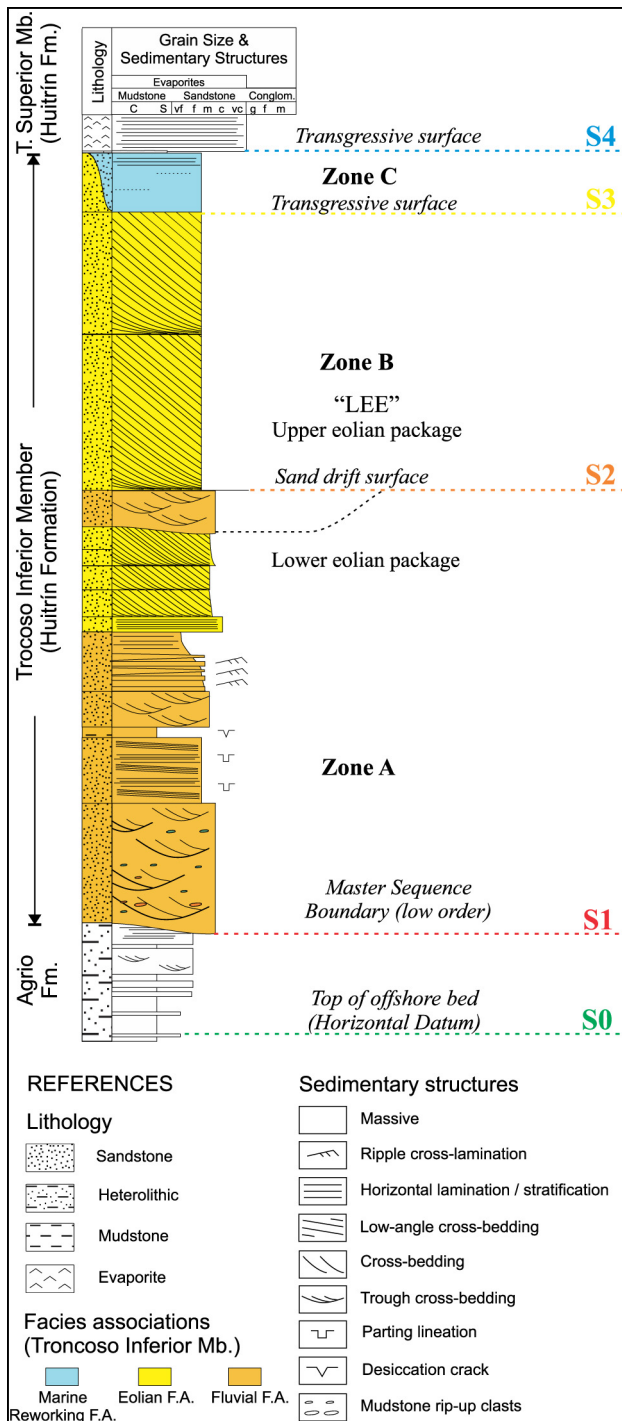


Figure 9. Detailed stratigraphic framework for the Troncoso Inferior Member in study area. “S” stands for “surface” (as in S0 to S4).

the top by Surface 2 (Fig. 9). This surface marks the base of the LEE and is characterized by the local appearance of facies indicating deflation processes across the whole study area, therefore representing a sand drift surface (Clemmensen and Tirsgaard,

1990). Zone B represents the LEE, isolated from previous eolian events, and includes only sandstones of the eolian facies association. Surface 3 marks the upper boundary of the LEE from both resedimented deposits and evaporites of the Troncoso Superior Member (Fig. 9). Zone C groups the discontinuous but locally important resedimented deposits of the marine reworking facies association. Finally, Surface 4 is the upper limit of the studied interval and marks the boundary between the sandstones of the Troncoso Inferior Member and the evaporites of the Troncoso Superior Member. Over broad extensions, the deposits of Zone C are only a few centimeters thick, or directly wedge out. Where the deposits of Zone C are not present, Surfaces 3 and 4 merge.

MORPHOLOGICAL ANALYSIS

Surface geometry and interpretation

Mapping of the surfaces within the stratigraphic framework was first carried out on the deformed model. Surface 0 shows a very regular shape dipping gently to the southwest, with isodepth lines forming a wide arc over the whole study area (Fig. 10a). Surface 1 in contrast, is clearly much more irregular even if the regional dip observed in the previous surface is still easily distinguishable (Fig. 10b). Surface 2 in turn, has a shape similar to surface 0, as it is once again much more regular with the exception of a few local disturbances (Fig. 10c). Finally, Surface 3 shows regular but far more abrupt features than surface 1, superimposed to the general dip which is not evident at first sight (Fig. 10d). Given the relatively low thickness of Zone C, the overall general shape of Surface 4 is very similar to Surface 3.

Considering that Surface 0 represents an approximation of the outer-ramp sea-floor gradient ($\ll 1^\circ$), its present dip can be considered as the tectonic deformation in this area. Taking this assumption, the shape of the isodepth lines in this surface is showing a very open syncline with an axis dipping 5° to the S-SW, which is compatible with the structural geology surrounding the study area. When comparing Surface 0 to Surface 2, it is clear that their geometries are very similar, which indicates that Surface 2 was very close to the horizontal at the time of its formation as well. This has important implications since it suggests that the dunes of the LEE

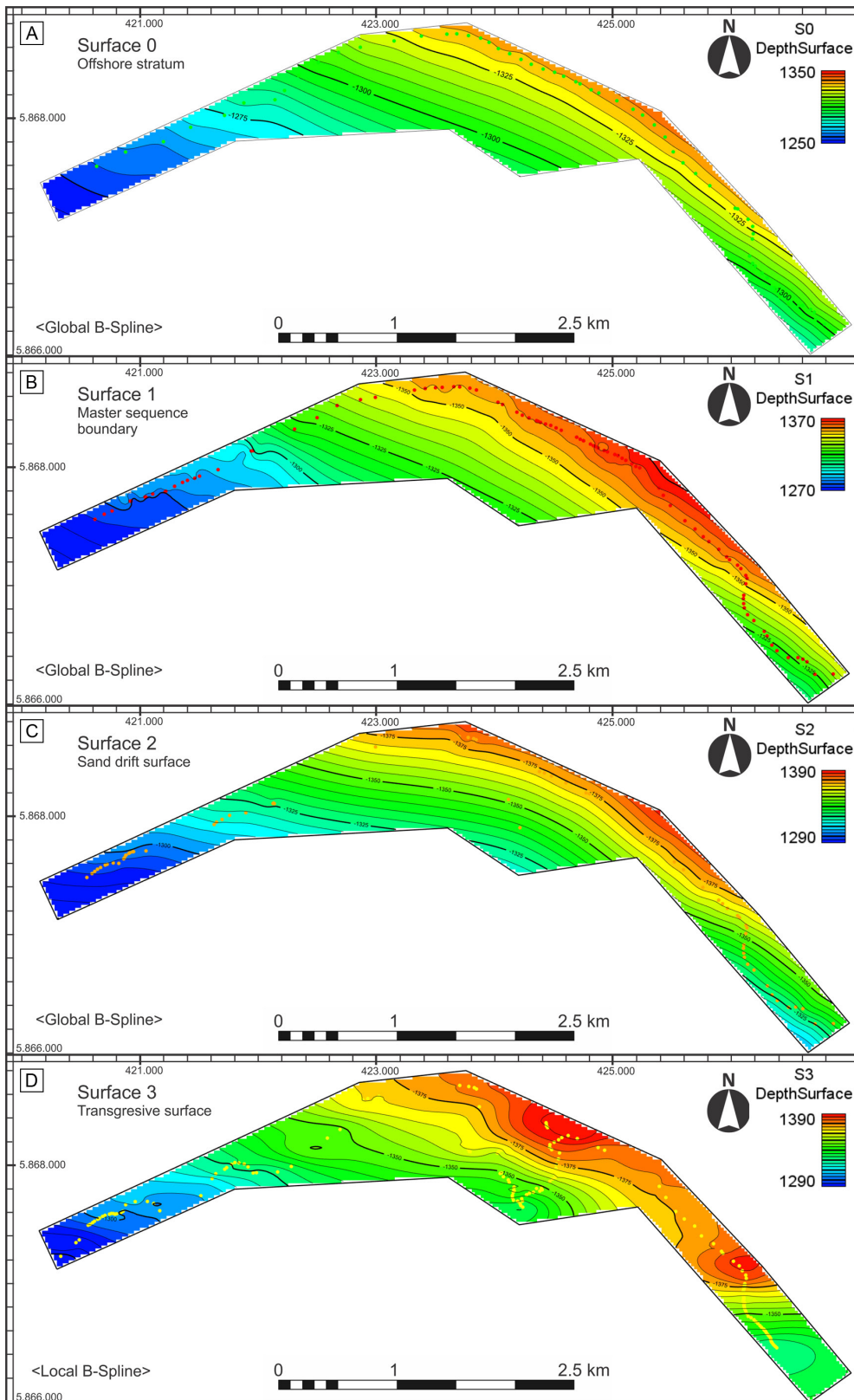


Figure 10. Results of surface mapping in the deformed model using RMS© software. Height values are expressed in meters above sea level. All surfaces are colored in a range of 100 meters to make the morphological analysis more objective.

were constructed over a relatively flat surface, and that a thickness map of Zone B should successfully reflect the preserved morphology of the dunes. The

irregularities observed in surfaces 1 and 3 in turn, most likely come from the erosion generated at the sequence boundary and the preserved morphology

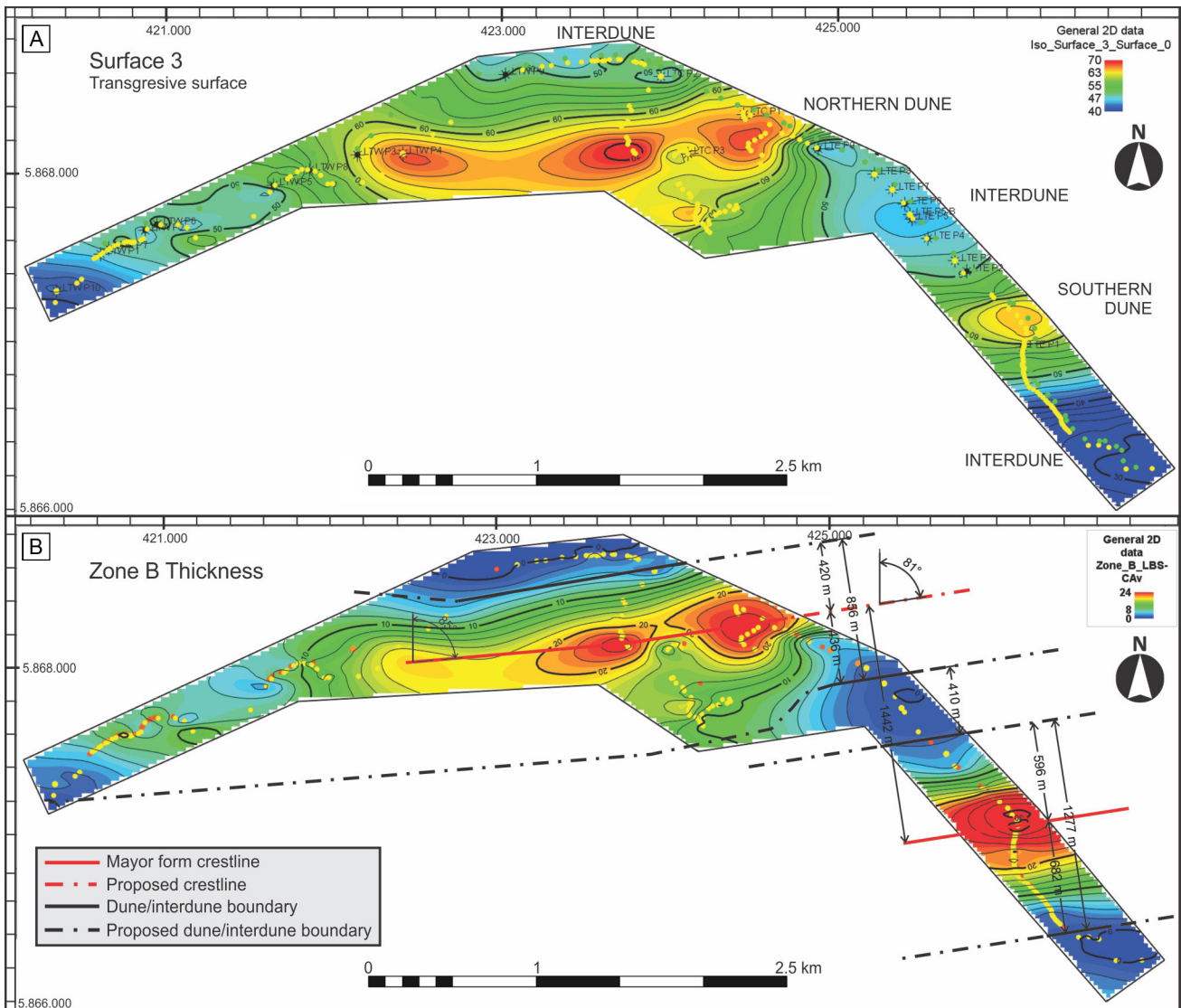


Figure 11. Analysis of thickness and depth surfaces within the retro-deformed model which are indicative of the preserved eolian morphology **a)** Surface 3 morphology with respect to surface 0 (horizontal datum), values expressed are meters above surface 0. **b)** Zone B thickness map, regarded as the most suitable for morphological analysis, portraying the results of large scale feature characterization, see text for discussion.

of the eolian dunes, respectively.

Characterization of the last eolian event

To characterize the preserved eolian morphology of the last eolian event, the depth map of Surface 3 and the thickness map of Zone B in the retro-deformed model were taken into account (Fig. 11). The realizations in the retro-deformed model allowed reducing the component of tectonic deformation in the mapping algorithms, thus providing more realistic results of the original morphology of this succession. Two large ridges of eolian sandstone are

observed, one to the north of the study area which was named “northern dune” and a second one to the southeast termed “southern dune” (Fig. 11a). Both features seem to have a general E-W orientation and are separated by an interdune sector in which the LEE thickness is reduced to a few centimeters or is not present at all (Fig. 11b). The limit between dune and interdune sectors was ultimately determined in the field by the presence or absence of large-scale cross-bedded facies, for which sedimentary logs and correlation photomosaics were critical. Both ridges have very broad, slightly convex-upward crestal areas with a sharp contact to the more steeply

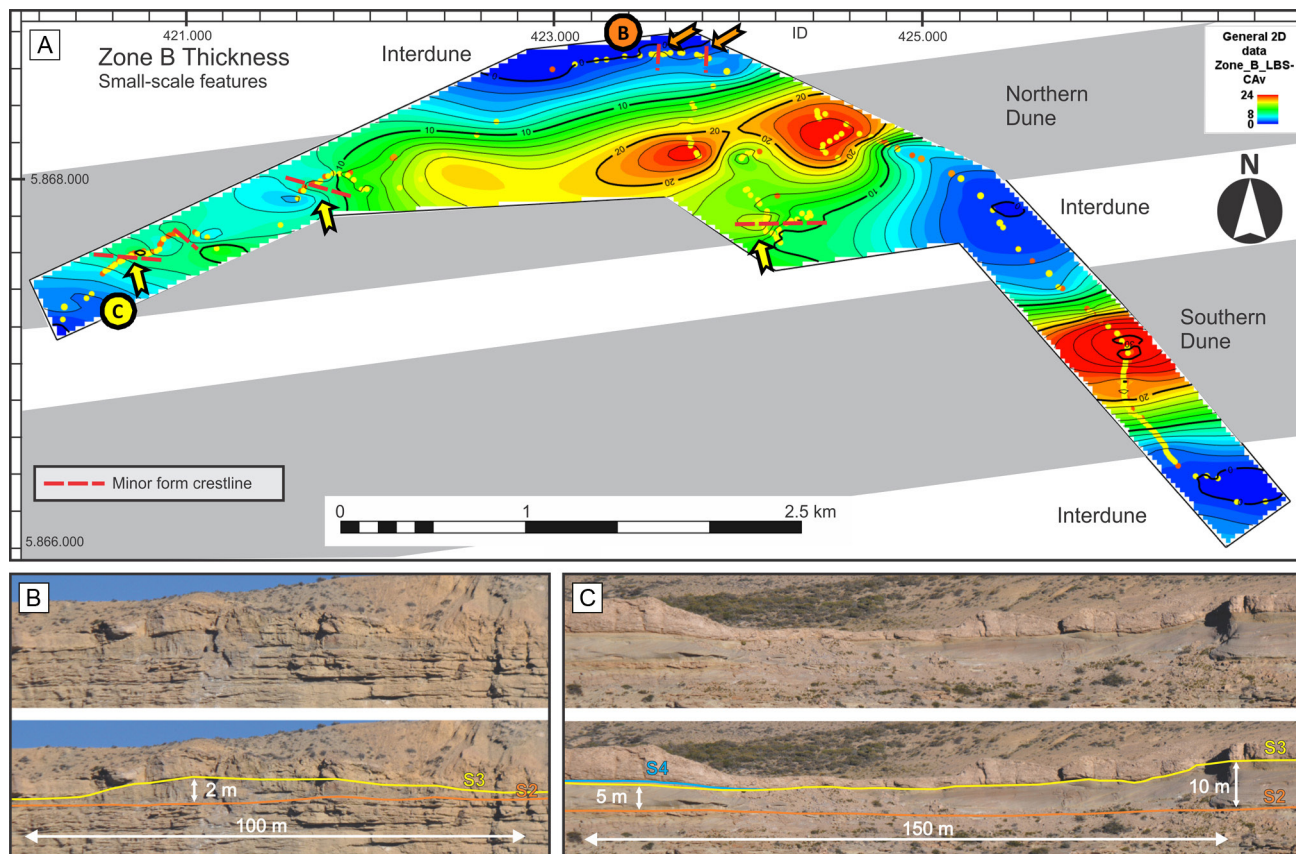


Figure 12. a) Zone B thickness map showing small-scale features analysis. Two broad types of features are indicated with orange and yellow arrows (see text for discussion). b) Example of a small-scale feature observed in the interdune area. c) Example of a small-scale feature within the major dune area. The location of both examples is indicated in figure 12a.

inclined flanks of concave shape, which gradually pass down into interdune sectors. Resedimented deposits seem to be more important in thickness and extension in the southern flanks of both ridges. They are almost absent in crestral areas and rapidly increase thickness in ridge flanks, but they usually reach interdune sectors with variable thickness.

Crest orientation was determined in the northern dune, where more data was available, giving an average N83-263° trend. Using this orientation, the dune crests and the boundaries between dune and interdune sectors were projected in order to perform measurements perpendicular to the bedform crests (Fig. 11b). Results show that the southern dune was significantly wider and higher than the northern one. The width of the ridges was measured in approximately 860 m for the northern dune and 1280 m for the southern dune. The preserved height was 24 and 31 m in the northern and southern dunes, respectively. Both ridges have a symmetric

cross section specially the northern one (symmetry index of 1.04 and 1.14 for the northern and southern dune, respectively), even though for both cases the southern flank is slightly longer than its northern counterpart. The spacing between crests is 1440 m, leaving an interdune area width of approximately 410 m.

Smaller-scale features were detected superimposed on the large-scale scheme. These were apparent in the generated maps and identified in outcrop (Fig. 12), and were separated into two different types. The most clearly discernible forms are oriented subperpendicular to the large ridges, have a height of 1-2 m, a clearly asymmetric section, and were observed in interdune areas (Fig. 12b). A second type of feature seems to be oriented subparallel to the main forms (Fig. 12c), even though a difference in orientation is noticeable, with a relief reaching up to 6 m and only found in the southern flank of the northern dune.

DISCUSSION AND ANALOGIES

The two large ridges of eolian sand represent the main bedforms of the last eolian system of the Troncoso Inferior Member in the study area. Small-scale features on the southern flank of the northern dune suggest that these larger forms were at some point draa, with smaller superimposed dunes in at least one of their flanks (Wilson, 1972). One possible explanation as to why the superimposed dunes are not ubiquitous in the dune area is that marine reworking during the flooding event most likely washed away the upper parts of the main bedforms. This gives the preserved wide and rounded nature of the crestral areas, free of reworked facies and surrounded by dune flanks with the thickest resedimented deposits. The adjacent interdune areas were characterized by very thin deposits (up to a few tens of centimeters), or by no deposition at all. The sandstone facies comprising these interdune deposits have no clear indicators of interaction with water during its formation (Fig. 6) and were likely deposited under dominantly dry conditions, well above the water table. In addition, small features subperpendicular to the major forms were also found in these sectors, and interpreted as smaller dunes developed in interdune areas.

Taking into account the symmetry of the main bedforms determined in this study, and evidence of their great continuity and straight form both in the Loma la Torre outcrops and in the subsurface sector to the east of the study area (Dajczgewand *et al.*, 2006), it is clear that these bedforms were dunes or draa of linear morphology. This type of dunes have been traditionally linked to low sand supply conditions and bimodal wind regimes (Wasson and Hyde, 1983).

A previous study in this area analyzed the basic internal sedimentary architecture of the eolian dunes (see figures 6 and 7 of Strömbäck *et al.*, 2005) in order to determine the past dynamics of these draa. That study highlighted the presence of large-scale cross bedding sets separated by second- and third-order bounding surfaces and an important bimodality in foreset dip directions (towards the north and east). Our own paleocurrent data taken from the last eolian event in the northern dune, shows this same tendency (Fig. 13). Preliminary architectural analysis shows internal bounding surfaces in dune areas dipping to the N in northern flanks and to the SE in

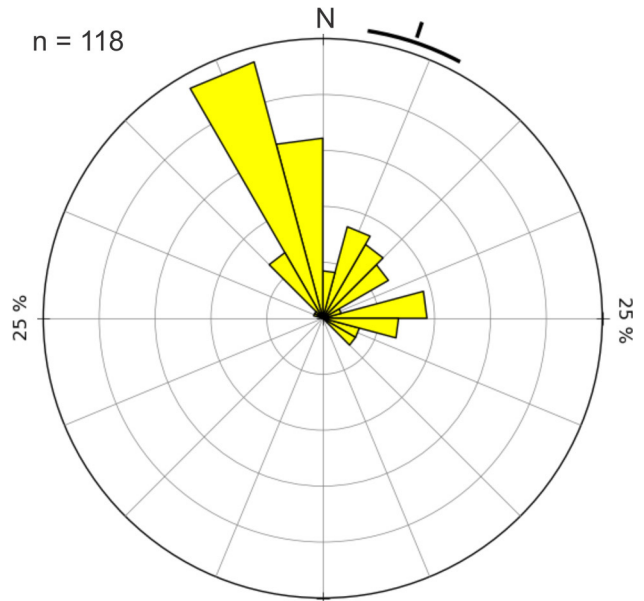


Figure 13. Rose diagram of the cross bedding dip directions for the last eolian event in the northern dune.

southern flanks. This evidence suggests a possible longitudinal behavior for the main bedforms of this sector, which is coherent with the observed linear morphology.

Given that the facies which characterize the interdune area lack evident indicators of deposition under humid conditions (Kocurek, 1981); an interpretation of a dry eolian system in the sense of Kocurek and Havholm (1993) prior to the flooding is supported. Dunes seem to have undergone construction under dominantly dry conditions coexisting with interdune sectors characterized by erosion and reduced sand accumulation. This also supports the idea of an abrupt transgression, instantaneous in geologic time scales, considering the lack of evidence for a rising water table, as would be expected from a gradual flooding of the basin (e.g. the Avilé Member of the Agrío Formation, Veiga *et al.*, 2002). Additionally, given the absence of a uniform preserved record in the interdune areas, it is clear that this system was not undergoing accumulation in this area, probably as a consequence of an insufficient sand supply or availability (Kocurek and Havholm, 1993).

To test if a system with the morphology and scale measured in the Troncoso Member is likely to develop, modern analogs were investigated. A sector of the southern Namib Sand Sea in western

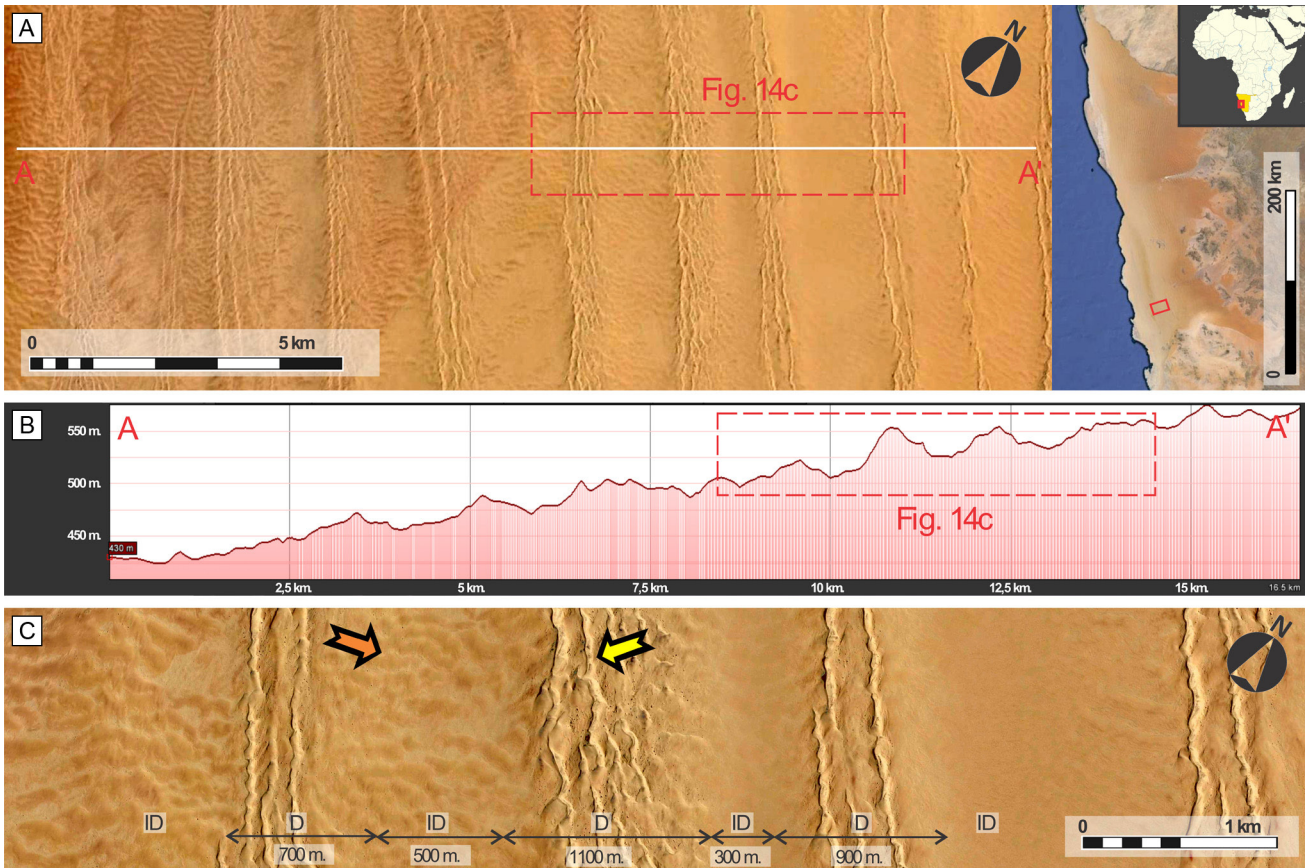


Figure 14. Modern analog. **a)** Compound linear bedforms (Livingstone, 2013), as seen from Google Earth imagery, in the southern Namib Sand Sea, Namibia, Africa (26°2'41.55" S; 15°16'0.40" E). **b)** Height and spacing of the major bedforms as showed by an elevation profile from SRTM data. **c)** Smaller scale dunes superimposed and oriented subparallel to the major bedforms (yellow arrow), along with small ridges oriented subperpendicular to the major bedforms and located in interdune areas (orange arrow). Width of the major bedforms (D) and their associated interdunes (ID) are shown as well.

Namibia, Africa, exhibits dunes with a morphology and scale similar to that reported for the Troncoso dunes (Fig. 14a). According to SRTM data along a 16-km-long transect, these draa have a height of 25-35 m relative to their surrounding interdunes and an average spacing of 1550 m (Fig. 14b). From Google Earth imagery, sets of superimposed bedforms with an orientation subparallel to the larger forms were observed. Moreover, small bedforms in the interdune area with an orientation subperpendicular to the draa are also apparent (Fig. 14c). The draa in this sector have been classified as compound linear forms by Livingstone (2013). This sector, as most of the central section of the Namib Sand Sea, is subjected to a seasonal, bimodal wind regime comprising southwesterly summer winds blowing from the Atlantic Ocean and easterly winter winds from inland South Africa (the so called "Berg" or

mountain winds - Livingstone, 2013). In addition, linear dunes in this sector have a relatively limited sand supply when compared to bigger bedforms in the northern erg sector, considering the equivalent sand thickness maps generated by Bullard *et al.* (2011).

Regarding the importance of this case as a subsurface analog, it is necessary to highlight that the identification of the different eolian sequences was critical for a precise morphological reconstruction of this interval. If the entire thickness of eolian deposits had been interpreted as the sequence preserved during subsequent flooding, the vertical precision of the reconstruction would have been diminished, causing variations in the results of the morphological characterization (compare the two scenarios shown in Fig. 15). In addition, failing to differentiate these sequences in the subsurface might lead, for

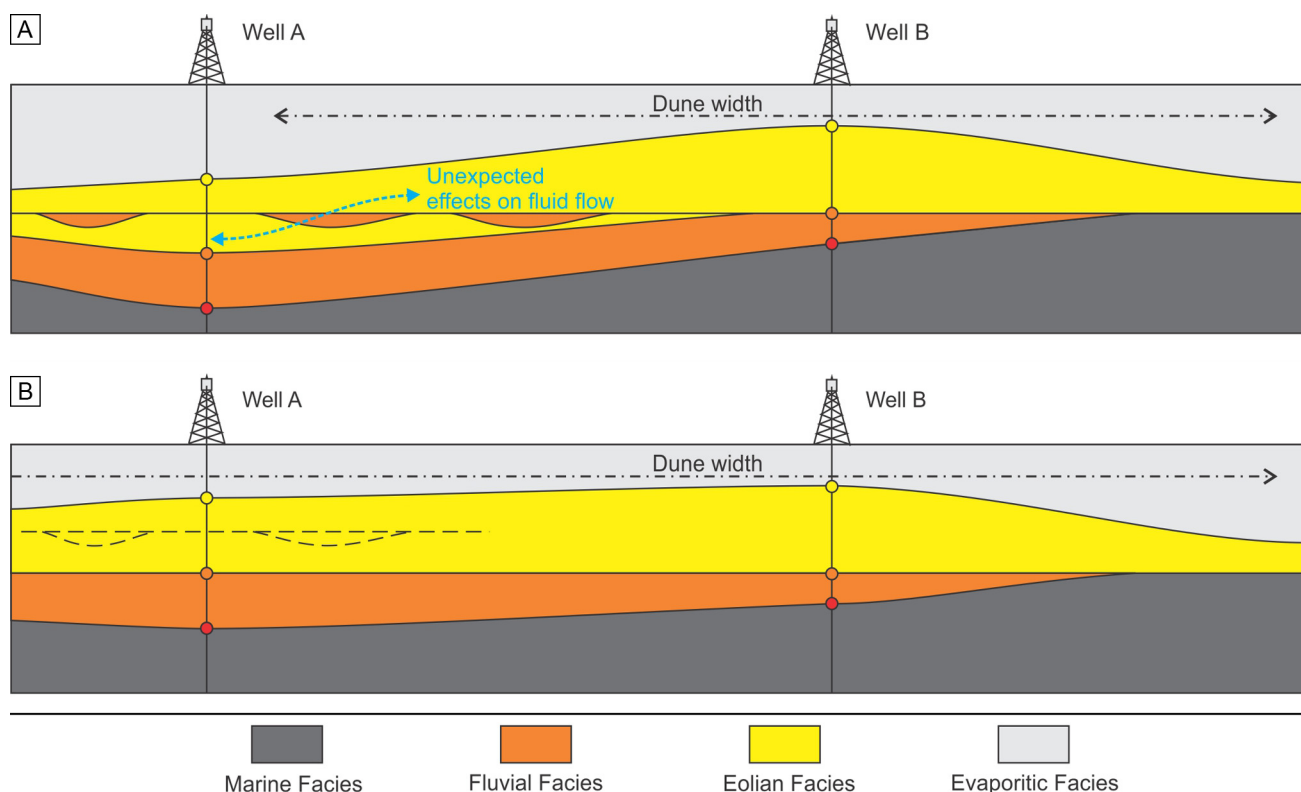


Figure 15. Possible interpretations for the same drilled sequence in a hypothetical subsurface scenario for the Troncoso Inferior Member. Note the impact in the reconstruction of the preserved eolian morphology and in the uncertainty in the distribution of sedimentary heterogeneity. **a)** Interpretation considering the presence of multiple eolian sequences. **b)** Interpretation failing to differentiate between different eolian sequences.

example, to underestimate the presence of changes in petrophysical properties caused by various types of fluvial deposits that are present between the two eolian sequences. Moreover, it is important to highlight that models of this unit which are tested for realistic proportions have a better opportunity to represent more accurately the geometry of this reservoir in the subsurface.

CONCLUSIONS

The elaboration of a detailed stratigraphic framework of the Troncoso Inferior Member in the Loma La Torre area was successful in identifying multiple independent eolian sequences and allowed the isolation of the last eolian event, responsible for generating the morphology preserved by the flooding associated to the development of the Troncoso Superior Member. A combination of several surveying methods, most importantly total station and 3D photogrammetry-based models, proved critical for the precise mapping of the stratigraphy across a vast area.

Morphological characterization of the preserved geometry of the last eolian event reveals a system of dunes and draa most likely of linear type and a nearly WSW-ENE orientation. Two major bedforms were identified in the study area. Morphological measurements in these forms show a preserved height of 24 and 31 m, an average width close to a kilometer, a symmetrical section and a dune spacing of 1450 m. Interdune sectors record very little, if any, deposition, and a measured width of approximately 400 meters. Small dunes were observed both in interdune areas and superimposed in the dune areas.

Taking into account modern analogs for the Troncoso dunes and considering the characteristics of interdune areas, it was determined that this system underwent construction under dry conditions and a limited supply or availability of sand, most likely under a bimodal wind regime. Immediately prior to the flooding, this system was not influenced by the water table and was not undergoing accumulation, owing its preservation entirely to the marine transgression.

The results indicate that modeling this unit in the subsurface with the detail required for managing mature fields, requires an excellent understanding of the system evolution at that locality, particularly to determine the presence of multiple eolian sequences.

Acknowledgments

This research was funded by the Consejo Nacional de Investigaciones Científicas y Técnicas (CONICET-PIP 112-201101-00322) and through a co-operation between YPF S.A. and CIG. Roxar Inc. is thanked for providing RMS© licenses. The authors wish to thank reviewers Giorgio Basilici and Claiton Scherer for their suggestions which considerably improved this manuscript. We are also grateful to Nicolas Scivetti, Mariana Olivo, Ignacio Escobar and Luciano Zapata for their assistance in the field and Martin Muravchik for providing software and rising awareness to the CIG community about the potential in experimenting with photogrammetric methods.

REFERENCES

- Al-Masrahy, M.A. and N.P. Mountney, 2013. Remote sensing of spatial variability in aeolian dune and interdune morphology in the Rub' Al-Khali, Saudi Arabia. *Aeolian Research* 11:155-170.
- Benan, C.A.A. and G. Kocurek, 2000. Catastrophic flooding of an aeolian dune field: Jurassic Entrada and Todilto Formations, Ghost Ranch, New Mexico, USA. *Sedimentology* 47:1069-1080.
- Bullard, J.E., K. White and I. Livingstone, 2011. Morphometric analysis of aeolian bedforms in the Namib Sand Sea using ASTER data. *Earth Surface Processes and Landforms* 36:1534-1549.
- Cignoni, P., M. Corsini and G. Ranzuglia, 2008. MeshLab: an open-source 3D mesh processing system. *ERCIM News* 73:45-46.
- Clemmensen, L.B., 1989. Preservation of interdune and plinth deposits by the lateral migration of large linear draas (Lower Permian Yellow Sands, northeast England). *Sedimentary Geology* 65:139-151.
- Clemmensen, L.B. and H. Tirsgaard, 1990. Sand-drift surfaces: A neglected type of bounding surface. *Geology* 18:1142-1145.
- Dajczgewand, D., A. Nocioni, M. Fantin, S. Minniti, R. Calegari and A. Gavarrino, 2006. Lower Troncoso aeolian bodies identification in the Neuquén Basin, Argentina: A different approach and some geological implications. *IX Simposio Bolivariano - Exploración Petrolera en las Cuencas Subandinas* Actas in CD, Cartagena, Colombia.
- Glennie, K.W. and A.T. Buller, 1983. The Permian Weissliegend of NW Europe—the partial deformation of aeolian dune sands caused by the Zechstein Transgression. *Sedimentary Geology* 35:43-81.
- Howell, J.A., E. Schwarz, L.A. Spalletti and G.D. Veiga, 2005. The Neuquén Basin: an overview. In G.D. Veiga, L.A. Spalletti, J.A. Howell and E. Schwarz (Eds.), *The Neuquén Basin: a case study in sequence stratigraphy and basin dynamics*. Geological Society of London, Special Publication 252:1-14.
- Howell, J.A., Å. Vassel and T. Aune, 2008. Modelling of dipping clinoform barriers within deltaic outcrop analogues from the Cretaceous Western Interior Basin, USA. In J. Griffiths, J. Hegre, A. Robinson and S. Price (Eds.), *The Future of Geological Modelling in Hydrocarbon Development*. Geological Society of London, Special Publication 309:99-121.
- Hunter, R.E., 1977. Basic types of stratification in small eolian dunes. *Sedimentology* 24:361-387.
- Jerram, D.A., N.P. Mountney, J.A. Howell, D. Long and H. Stollhofen, 2000. Death of a sand sea: an active aeolian erg systematically buried by the Etendeka flood basalts of NW Namibia. *Journal of the Geological Society* 157:513-516.
- Kocurek, G., 1981. Significance of interdune deposits and bounding surfaces in aeolian dune sands. *Sedimentology* 28:753-780.
- Kocurek, G. and K.G. Havholm, 1993. Aeolian sequence stratigraphy—a conceptual framework. In P. Weimer, and H.W. Posamentier (Eds.), *Siciliclastic Sequence Stratigraphy*. American Association of Petroleum Geologists, Memoir 58:393-409.
- Legarreta, L., 2002. Eventos de desecación en la Cuenca Neuquina: depósitos continentales y distribución de hidrocarburos. *V Congreso de Exploración y Desarrollo de Hidrocarburos* Actas en CD, Mar del Plata, Argentina.
- Livingstone, I., 2013. Aeolian geomorphology of the Namib Sand Sea. *Journal of Arid Environments* 93:30-39.
- Masarik, M.C., 2002. Los reservorios del Miembro Troncoso Inferior de la Formación Huitrín. In M. Schiuma, G. Hinterwimmer and G. Vergani (Eds.), *Rocas reservorio de las cuencas productivas de la Argentina*: 465-492.
- Scherer, C.M.S., 2002. Preservation of aeolian genetic units by lava flows in the Lower Cretaceous of the Paraná Basin, southern Brazil. *Sedimentology* 49:97-116.
- Spalletti, L.A., D.G. Poiré, E. Schwarz and G.D. Veiga, 2001. Sedimentologic and sequence stratigraphic model of a Neocomian marine carbonate-siliciclastic ramp: Neuquén Basin, Argentina. *Journal of South American Earth Sciences* 14:609-620.
- Strömbäck, A. and J.A. Howell, 2002. Predicting distribution of remobilized aeolian facies using sub-surface data: the Weissliegend of the UK Southern North Sea. *Petroleum Geoscience* 8:237-249.
- Strömbäck, A., J.A. Howell and G.D. Veiga, 2005. The transgression of an erg – sedimentation and reworking/soft-sediment deformation of aeolian facies: the Cretaceous Troncoso Member, Neuquén Basin, Argentina. In G.D. Veiga, L.A. Spalletti, J.A. Howell and E. Schwarz (Eds.) *The Neuquén Basin: a case study in sequence stratigraphy and basin dynamics*. Geological Society of London, Special Publication 252:163-183.
- Valenzuela, M.E., R. Córeron, M.C. Masarik and M.D. Vallejo, 2011. Yacimientos Chihuido de la Sierra Negra-Lomita-Lomita Norte y El Trapial. In H.A. Leanza, C. Arregui, E. Carbone, J.C. Danieli and J. Vallés (Eds.) *Geología y Recursos Naturales de la Provincia del Neuquén*:677-687.
- Veiga, G.D. and G.D. Vergani, 2011. El Miembro Troncoso Inferior de la Formación Huitrín (Cretácico Temprano). In H.A. Leanza, C. Arregui, E. Carbone, J.C. Danieli and J. Vallés (Eds.)

Geología y Recursos Naturales de la Provincia del Neuquén: 181-188.

Veiga, G.D., L.A. Spalletti and S. Flint, 2002. Aeolian/fluvial interactions and high resolution sequence stratigraphy of a non-marine lowstand wedge: The Avilé Member of the Agrio Formation (Lower Cretaceous) in central Neuquén Basin, Argentina. *Sedimentology* 49:1001-1019.

Veiga, G.D., J.A. Howell and A. Strömbäck, 2005. Anatomy of a mixed marine/non-marine lowstand wedge in a ramp setting. The record of a Barremian/Aptian complex relative sea-level fall in Central Neuquén Basin, Argentina. In G.D. Veiga, L.A. Spalletti, J.A. Howell and E. Schwarz (Eds.) *The Neuquén Basin: a case study in sequence stratigraphy and basin*

dynamics. Geological Society of London, Special Publication 252:139-162.

Vergani, G.D., M. Barrionuevo, H. Sosa and M. Pedrazzini, 2001. Análisis estratigráfico secuencial de alta resolución en la Formaciones Agrio y Huitrín en el Yacimiento Puesto Hernández, Cuenca Neuquina, Argentina. *Boletín de Informaciones Petroleras* 67:76-87.

Wasson, R.J. and R. Hyde, 1983. Factors determining desert dune type. *Nature* 304:337-339.

Wilson, I.G., 1972. Aeolian bedforms – their development and origins. *Sedimentology* 19:173-210.

Wu, C., 2011. VisualSFM: A Visual Structure from Motion System. <http://ccwu.me/vsfm/>.